13,03

SiC thermal conductivity: calculation of the isotope effect from first principles

© D.A. Chernodoubov, A.V. Inyushkin

National Research Center „Kurchatov Institute“,
Moscow, Russia

E-mail: Chernodubov_DA@nrcki.ru

Received April 14, 2023
Revised April 14, 2023
Accepted May 6, 2023

The thermal conductivity temperature dependence $\kappa(T)$ of a hexagonal 2*H*-SiC silicon carbide crystal was calculated using the first-principle approach for the orientation of the heat flux in the basal plane and along the hexagonal axis *c* in the temperature range from 100 to 500 K. The effect of silicon and carbon isotopic disorder on thermal conductivity is considered. It was found that, at a temperature of 300 K, the thermal conductivity of isotopically pure 2*H*-SiC containing 100% ^{28}Si and 100% ^{12}C is higher by 15.2% and 12.4% for directions along and across the basal plane, respectively, than that of crystals with a natural composition of silicon and carbon isotopes. For crystals with a natural mixture of carbon isotopes ^{textnat}C, the isotope effect for silicon is 14.5% and 11.9% for these directions.

Keywords: single crystal, thermal conductivity, silicon carbide, first principle calculation.

DOI: 10.21883/PSS.2023.06.56120.62

1. Introduction

SiC is included in a small wide-band semiconductor group with thermal conductivity higher than that of copper [1]. High thermal conductivity of SiC, besides other outstanding electronic and optical properties, makes it a very attractive material for high-frequency and power electronics and for optical applications [2,3]. Silicon carbide has more than 200 polytype modifications such as cubic 3*C*-SiC, hexagonal 4*H*- and 6*H*-SiC andrhombohedral 15*R*- and 21*R*-SiC. Thermal conductivity was studied experimentally and theoretically for a limited set of polytypes — 3*C*-SiC, 4*H*- and 6*H*-SiC whose bulk crystals are available for practical applications. The most pure SiC crystals exhibit temperature dependence $\kappa(T)$ typical for normal crystalline dielectrics with phonon thermal conductivity mechanism [1]. At relatively high temperatures, including room temperature, $\kappa(T)$ increases with temperature decrease due to reduced contribution of anharmonic phonon-phonon processes to the total phonon scattering rate. At low temperature, thermal conductivity achieves its maximum. The phonon-phonon process rate is comparable with the scattering rate on point defects and sample boundaries at this point. „Impurity isotopes“ of elements forming the compound as well as chemical impurities and structural defects of lattice (vacancies, interstices, etc.) are classified as point defects. Impurity isotopes with atomic weights different from the matrix atomic weight are randomly distributed over the lattice sites. This destroys translation symmetry of the crystal resulting in isotopic phonon scattering. This scattering may considerably reduce thermal conductivity of pure crystals (see, for example, [4]).

Many elements forming the semiconductors have two and more stable isotopes. For example, natural composition of silicon isotopes ^{nat}Si contains 92.223% ^{28}Si, 4.685% ^{29}Si and 3.092% ^{30}Si. ^{nat}C with natural composition includes 98.93% ^{12}C and 1.07% ^{13}C. The experiments have shown that even such small ^{13}C „impurity“ causes dramatic reduction, approximately by 50%, of thermal conductivity of diamond compared with crystal enriched in ^{12}C up to 99.93% at room temperature [5–7]. High lattice stiffness, low anharmonicity and relatively high isotope weight difference cause such heavy isotopic effect in diamond. In the crystalline silicon, „impurity“ ^{29}Si and ^{30}Si reduce thermal conductivity by 8% according to the measurements [8–10]. Silicon carbide is addressed in a paper [11] devoted to the experimental study of isotopic effect in thermal conductivity of 4*H*-SiC SiC polytype. Samples in the form of 75 μm films with ^{28}Si and ^{12}C concentration up to 99.5% were obtained by the CVD method on 4*H*-SiC crystalline substrates. Their thermal conductivity along the hexagonal axis *c* was measured by the transient thermoreflectance method. Increase in thermal conductivity due to at least 18% enrichment was observed at a temperature slightly (several dozens degrees) higher than room temperature.

There are theoretical estimates of isotopic effect for some SiC polytypes. Thus, in [1,12], in the framework of Callaway's phenomenological theory, effect of 36% for an unspecified crystalline phase of SiC at 300 K was estimated. In the recent decades, a significant progress has been achieved in the thermal conductivity ab initio theory that does not involve additional empirical assumptions [13,14]. In particular, $\kappa(T)$ was calculated for silicon, germanium

and diamond and the results agree with the experimental data, including isotropic effect data. For the isotopic effect in silicon carbide, ab initio calculations have been published only for cubic 3*C*-SiC and have shown that this effect for silicon carbide is equal to 20% [14]. Recently, [15] has provided calculations of $\kappa(T)$ for 2*H*-, 4*H*- and 6*H*-SiC polytypes, but the isotopic effect has not been studied. This paper reports thermal conductivity calculations for 2*H*-SiC polytype within $100 < T < 500$ K, addresses different mixtures of silicon and carbon isotopes, discusses the influence of the isotopic disorder on the main components of the thermal conductivity tensor.

2. Computational methods

Thermal conductivity of hexagonal crystals is of anisotropic type described by a second-rank tensor with two, as a matter of fact, different diagonal components for directions along the hexagonal axis c and perpendicular to this axis, i.e. in the basal plane. Components are often named by their orientation with respect to this plane: the first component is designated as perpendicular (or *out-of-plane*) κ_{out} and the second component is designated as parallel (or *in-plane*) κ_{in}. Phonon thermal conductivity of silicon carbide was calculated by a procedure described in [15–18] using ShengBTE package [19]. Thermal conductivity of a crystal is calculated by the following expression (see, for example, [16]):

$$\kappa_{\alpha\beta} = \sum_{\lambda} C_{\lambda} v_{\lambda,\alpha} v_{\lambda,\beta} \tau_{\lambda,\beta}, \qquad (1)$$

where summation is over all phonon modes $\lambda \equiv (\mathbf{q}, j)$ with wave vector $\mathbf{q}$ and polarization j; C_{λ} is the specific (volumetric) heat capacity of phonon mode λ; $v_{\lambda,\alpha}$ is the group velocity of mode λ along direction α in the orthogonal (Cartrsian) axes, and τ_{λ} is the lifetime of mode λ. Phonon spectrum and phonon relaxation times in three-phonon scattering processes was calculated on $25\times25\times15$ grid of wave vectors in the Brillouin zone. Values calculated in [20] using QUANTUM ESPRESSO package [21] on $6\times6\times4$ primitive cell grid (576 atoms) were used as second-order power constants. Third-order interatomic power constants were calculated using a $3\times3\times3$ supercell (108 atoms) in [15]. Then, thermal conductivity values were calculated by solution of the Boltzmann transport equation taking into account three-phonon scattering processes and scattering on impurity isotopes, whereby complete solution correctly considers the difference between phonon-phonon normal (with quasi-momentum conservation) and resistive (with quasi-momentum umklapp scattering) processes.

In a polyatomic crystal, phonon scattering rate on isotopes randomly distributed over the lattice sites is calculated using the expression [22]

$$\tau_{\text{iso}}^{-1}(\lambda, \omega) = \frac{\pi}{2N} \omega^2(\lambda) \sum_{\lambda'} \delta\big(\omega(\lambda) - \omega(\lambda')\big) \times \sum_{\sigma} g(\sigma) \big|\mathbf{e}^*(\sigma, \lambda') \cdot \mathbf{e}(\sigma, \lambda)\big|^2, \qquad (2)$$

where N is the number of lattice cells in the crystal, and $\mathbf{e}(\sigma, \lambda)$ is the polarization vector of phonon mode λ and atom σ. Constant $g(\sigma)$ is an isotopic disorder parameter that determines the isotopic scattering rate:

$$g(\sigma) = \sum_{i} c_i(\sigma) \left(\frac{\Delta M_i(\sigma)}{\overline{M}(\sigma)} \right)^2, \qquad (3)$$

where $\Delta M_i(\sigma) = M_i(\sigma) - \overline{M}(\sigma)$, $M_i(\sigma)$ and $\overline{M}(\sigma)$ is the weight of the i-th isotope and average atomic weight σ, c_i is the i-th isotope concentration. The scattering rate in three-phonon processes and isotopic scattering rate are summed up in accordance with the Matthiessen's rule.

3. Findings and discussion

To the best of our knowledge, no experimental thermal conductivity data for 2*H*-SiC crystals are reported in the literature. We have compared our calculated dependences $\kappa_{\text{in}}(T)$ and $\kappa_{\text{out}}(T)$ with the findings in [15] for 2*H*-SiC with natural composition of silicon and carbon isotopes. Thermal conductivity values obtained herein are a little, within 5%, lower than those reported in [15]. Thus, at 300 K, our $\kappa_{\text{in}}(T) = 486$ W/(m K) is approx. 4% lower, and for $\kappa_{\text{out}}(T) = 435$ W/(m K) — is 2% lower. In both papers, the Boltzmann equation was solved by the iteration method using ShengBTE package [19]. A minor discrepancy is possibly attributed to different criteria used to stop the iteration process.

Thermal conductivity $\kappa_{\text{in}}(T)$ along the basal plane is higher than along the axis c. Anisotropy is about 11.6% for a crystal with natural isotropic composition, but is a little higher, 14.4% for monoisotopic crystal at 300 K.

Figure 1 shows the thermal conductivity calculation results for 2*H*-SiC with two compositions of silicon and carbon isotopes — natural $\kappa_{\text{in,out}}^{(\text{nat})}(T)$ and monoisotopic, composed of 100% ^{28}Si and ^{12}C, $\kappa_{\text{in,out}}^{(2812)}(T)$. For both directions in he crystal, an expected result was achieved — crystal with lower isotopic disorder has higher thermal conductivity. The isotopic effect, i.e. ratio of thermal conductivity of a monoisotopic crystal and thermal conductivity of a crystal with natural composition $\kappa^{(2812)}(T)/\kappa^{(\text{nat})}(T) - 1$, grows with decreasing temperature (see Figure 2), whereby the effect is higher for $\kappa_{\text{in}}(T)$. At room temperature, the effect is 15.2% for $\kappa_{\text{in}}(T)$ and 12.4% for $\kappa_{\text{out}}(T)$. The values obtained for hexagonal 2*H*-SiC are much lower, by 20%, than the theoretically predicted values for cubic 3*C*-SiC [14]. According to calculations [15], thermal conductivity of SiC decreases in a row 2*H*, 4*H*, 6*H*. This is associated with the

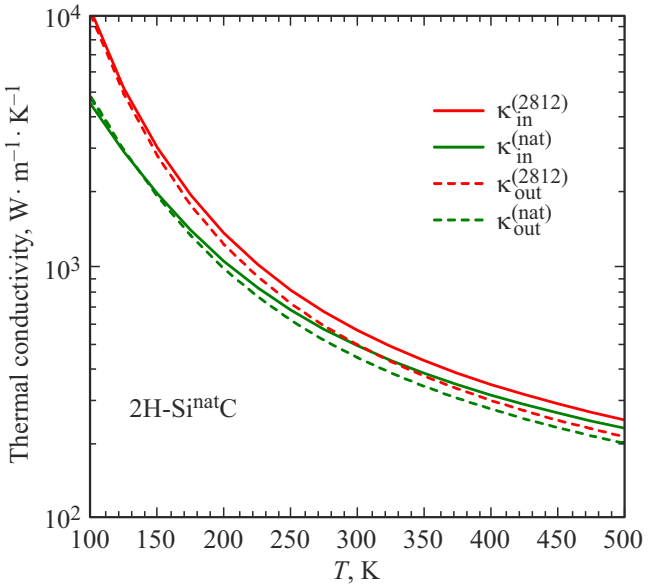

Figure 1. Temperature dependence of thermal conductivity components $\kappa_{in}(T)$ and $\kappa_{out}(T)$ for 2*H*-SiC with natural and monoisotopic element compositions. Solid lines correspond to $\kappa_{in}(T)$, dashed lines correspond to $\kappa_{out}(T)$. Red lines show the data for the monoisotopic composition ($^{28}Si^{12}C$), and green lines show the natural composition $^{nat}Si^{nat}C$.

fact that with growing number of atoms in the lattice cell in these crystals, the number of low-frequency optical branches (having low group velocities) of the phonon spectrum increases, and the interval between the acoustic and optical phonon frequencies decreases [15]. All this results in an increase in the acoustic phonon scattering rate in phonon-phonon processes.

As a result, the isotopic effect defined by the ratio of scattering rate in phonon-phonon processes and isotopic scattering rate is expected to decrease in the row 2*H*, 4*H*, 6*H*. In case of 2*H*-SiC, increase in the isotopic effect with temperature reduction is caused by relatively considerable reduction of contribution of three-phonon processes (primarily — due to „freezing out" of umklapp scattering processes) to thermal conductivity compared with the isotopic scattering contribution.

With growing isotopic disorder $g(\mathrm{Si})$, the isotopic scattering rate grows and thermal conductivity decreases accordingly. This is illustrated in Figure 3. The figure shows relative variation of thermal conductivity normalized to a value for the natural isotopic composition of silicon depending on $g(\mathrm{Si})$ for the silicon sublattice (carbon sublattice has a natural composition of ^{nat}C). Maximum value of $g(\mathrm{Si}) \approx 1187$ corresponds to 50% ^{28}Si and 50% ^{30}Si. The following interesting result shall be noted — the given thermal conductivity variation range is wider for component κ_{in}. This may indicate that the relative contribution of isotopic scattering to thermal conductivity κ_{in} is higher compared with the contribution of three-phonon processes than for κ_{out}. This agrees with a lower κ_{out} compared with κ_{in} (see Figure 1 and Figure 2).

Figure 4 shows differential contribution $\kappa_{in}(\nu)$ of phonon modes to thermal conductivity κ_{in} depending on frequency of modes ν for crystals with different isotopic compositions. $\kappa_{in}^{(2812)}(\nu)$ is the thermal conductivity of phonon modes associated only with inherent three-phonon scattering processes, and $\kappa_{in}^{(28)}(\nu)$ — when additional phonon scattering

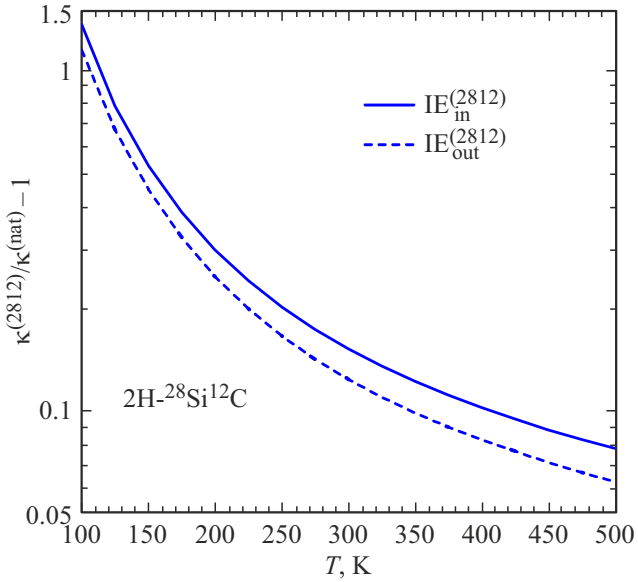

Figure 2. Isotopic effect $\kappa^{(28)}(T)/\kappa^{(nat)}(T) - 1$ as a function of temperature for 2*H*-SiC. Solid lines correspond to $\kappa_{in}(T)$, dashed lines correspond to $\kappa_{out}(T)$.

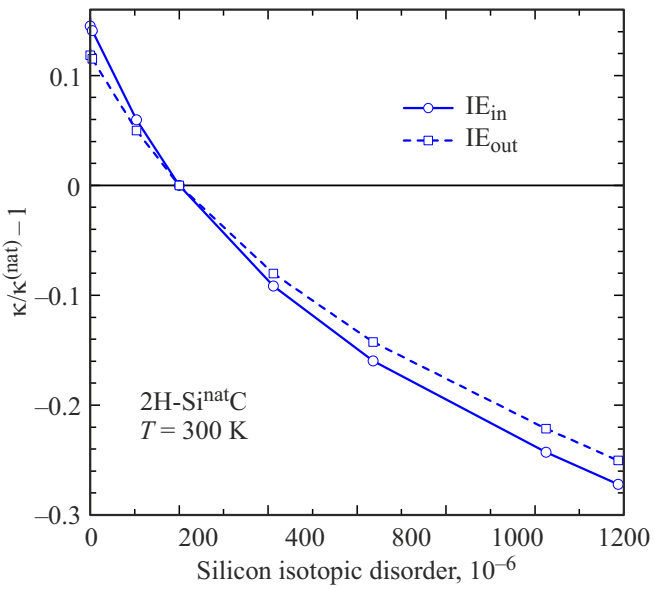

Figure 3. Dependence of the thermal conductivity tensor components for 2*H*-SiC on isotopic disorder constant $g(\mathrm{Si})$ at 300 K. thermal conductivity values normalized to the thermal conductivity of the crystal with natural composition of silicon isotopes are provided.

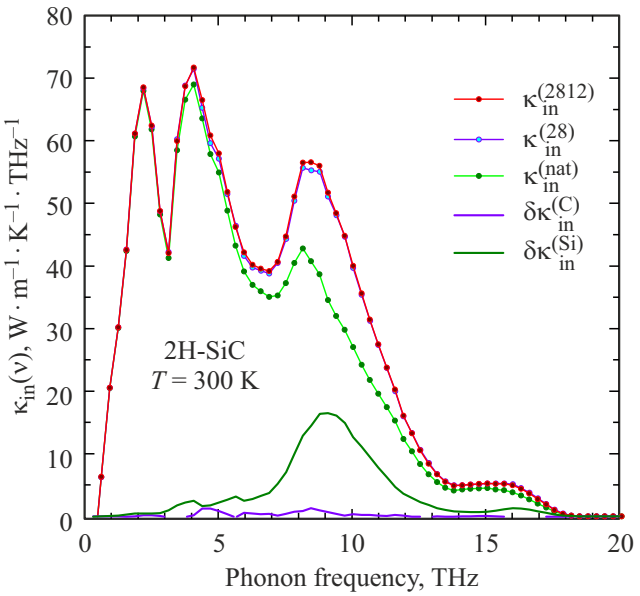

Figure 4. Dependence of differential contribution $\kappa_{in}(\nu)$ in κ_{in} for 2*H*-SiC on frequency ν of phonon modes at 300 K. Data for crystals with different isotopic compositions of silicon and carbon are shown.

is present on the carbon sublattice isotopes with natural composition ^{nat}C. $\kappa_{in}^{(nat)}(\nu)$ represents thermal conductivity of a crystal with natural isotope composition of both elements. Difference of these two values $\kappa_{in}^{(2812)}(\nu) - \kappa_{in}^{(28)}(\nu)$ represented by curve $\delta\kappa_{in}^{(C)}$ shows how much the thermal conductivity of phonon modes is reduced by scattering on carbon isotopes with natural composition. Whereas curve $\delta\kappa_{in}^{Si} = \kappa_{in}^{(28)}(\nu) - \kappa_{in}^{(nat)}(\nu)$ is the effect from „inclusion“ of scattering on silicon isotopes with natural composition.

Figure 4 shows that scattering on isotopes is has a negligibly minor influence on the thermal conductivity of phonon modes in the low-frequency spectrum up to 3 THz for the crystal with natural composition of isotopes. This is attributed to the fact that three-phonon processes in this frequency range scatter phonons 2 to 3 orders of magnitude more intensively than „impurity“ isotopes (see Figure 8 from [15]). With frequency growth, the isotopic scattering rate approaches the three-phonon process scattering rate. Moreover, phonon scattering on silicon isotopes, rather than on carbon isotopes, suppresses thermal conductivity. This scattering plays a substantial role for phonon frequencies approx. from 7 to 12 THz, where a peak of phonon state density is present.

The calculations have shown that thermal conductivity (integral) $\kappa_{in}^{(2812)}$ of monoisotopic two-element ^{28}Si^{12}C crystal is only approx. 0.6% higher than that of ^{28}Si^{nat}C crystal. Thus, the isotopic disorder by carbon negligibly reduces thermal conductivity κ_{in} at 300 K. This result is caused by two conditions. The first is that the isotopic disorder in the carbon subsystem is about 3 times lower than that in the silicon subsystem: $g(\mathrm{C}) = 73.9$, $g(\mathrm{Si}) = 200.7$. The second is that due to a low atomic weight of carbon, their wave vectors $\mathbf{e}(\mathrm{C}, \lambda)$ are considerably lower that those of silicon $\mathbf{e}(\mathrm{Si}, \lambda)$ in the range of acoustic phonons that dominate in thermal conductivity. Since the isotopic scattering rate depends on the wave vector (see equation (2), as the fourth power of the vector in case of a cubic crystal [23]), then this factor also considerably reduces the scattering efficiency on carbon isotopes. It should be also noted that the carbon isotopic effect in thermal conductivity κ_{out} is even lower and equals 0.5% at 300 K.

4. Conclusion

Calculations of thermal conductivity tensor components for 2*H*-SiC polytype silicon carbide crystal are presented for various silicon and carbon isotope compositions. In accordance with the published theoretical data, thermal conductivity along the hexagonal axis has been found to be lower than along the basal plane. Monoisotopic ^{28}Si^{12}C crystal has thermal conductivity higher by 15.2% and 12.4% than the crystal with natural mixtures of silicon and carbon isotopes, respectively, for $\kappa_{in}(T)$ and $\kappa_{out}(T)$ at 300 K. Higher isotopic effect for $\kappa_{in}(T)$ compared with $\kappa_{out}(T)$ and larger thermal conductivity variation range $\kappa_{in}(300\ \mathrm{K})$ when the isotopic composition is changed suggest a relatively high isotopic scattering contribution for the direction along the basal plane of the crystal. Contribution of scattering on carbon isotopes with natural composition to the thermal conductivity of monoisotopic ^{28}Si crystal is negligible and does not exceed 0.6% at room temperature. This is attributed both to low isotopic disorder in the carbon subsystem and to small polarization vectors of „light“ carbon (compared with silicon) in the low-frequency phonon spectrum region.

Acknowledgments

The authors are grateful to Nakib Haider Protik for the provided numerical data on third-order interatomic power constants for hexagonal SiC crystals.

Funding

The research was performed within the Thematic R & D Plan of National Research Center „Kurchatov Institute“ using the equipment provided by the resource centers.

Conflict of interest

The authors declare that they have no conflict of interest.

References

[1] D.T. Morelli, G.A. Slack. In: High Thermal Conductivity Materials / Ed. S.L. Shinde, J.S. Goela. Springer, N.Y. (2006). P. 37–68.

[2] S.E. Saddow, A.K. Agarwal. Advances in Silicon Carbide Processing and Applications. Artech House, Inc., Boston, London (2004). 212 p.
[3] J.S. Goela, N.E. Brese, L.E. Burns, M.A. Pickering. In: High Thermal Conductivity Materials / Ed. S.L. Shinde, J.S. Goela. Springer, N.Y. (2006). P. 167–198.
[4] A.P. Zhernov, A.V. Inyushkin. Phys. Usp. **45**, 527 (2002).
[5] T.R. Anthony, W.F. Banholzer, J.F. Fleischer, L. Wei, P.K. Kuo, R.L. Thomas, R.W. Pryor. Phys. Rev. B **42**, 1104 (1990).
[6] L. Wei, P.K. Kuo, R.L. Thomas, T.R. Anthony, W.F. Banholzer. Phys. Rev. Lett. **70**, 3764 (1993).
[7] A.A. Kaminsky, V.G. Ral'chenko, H. Eneda, A.P. Bolshakov, A.V. Inyushkin. Pisma v ZTEF, **104**, 356 (2016). (in Russian)
[8] A.V. Gusev, A.M. Gibin, O.N. Morozkin, V.A. Gavva, A.V. Mitin. Neorgan. materialy **38**, 1305 (2002). (in Russian).
[9] A.V. Inyushkin, A.N. Taldenkov, A.M. Gibin, A.V. Gusev, H.-J. Pohl. Phys. Status Solidi C **1**, 2995 (2004).
[10] A.V. Inyushkin, A.N. Taldenkov, I.J.W. Ager, E.E. Haller, H. Riemann, N.V. Abrosimov, H.-J. Pohl, P. Becker. J. Appl. Phys. **123**, 095112 (2018).
[11] B. Lundqvist, P. Raad, M. Yazdanfar, P. Stenberg, R. Liljedahl, P. Komarov, N. Rorsman, J. Ager, O. Kordina, I. Ivanov, E. Janzen. 19th Int. Workshop on Thermal Investigations of ICs and Systems (THERMINIC). (2013). 58−61 p.
[12] D.T. Morelli, J.P. Heremans, G.A. Slack. Phys. Rev. B **66**, 195304 (2002).
[13] D.A. Broido, M. Malorny, G. Birner, N. Mingo, D.A. Stewart. Appl. Phys. Lett. **91**, 231922 (2007).
[14] L. Lindsay, D.A. Broido, T.L. Reinecke. Phys. Rev. B **87**, 165201 (2013).
[15] N.H. Protik, A. Katre, L. Lindsay, J. Carrete, N. Mingo, D. Broido. Mater. Today Phys. **1**, 31 (2017).
[16] N.K. Ravichandran, D. Broido. Phys. Rev. B **98**, 085205 (2018).
[17] N.K. Ravichandran, D. Broido. Nat. Commun. **10**, 827 (2019).
[18] M. Fava, N.H. Protik, C. Li, N.K. Ravichandran, J. Carrete, A. van Roekeghem, G.K.H. Madsen, N. Mingo, D. Broido. npj Comput. Mater. **7**, 54 (2021).
[19] W. Li, J. Carrete, N.A. Katcho, N. Mingo. Comput. Phys. Commun. **185**, 1747 (2014).
[20] Y. Xie, J. Vandermause, S. Ramakers, N.H. Protik, A. Johansson, B. Kozinsky. npj Comput. Mater. **9**, 36. (2022).
[21] P. Giannozzi, O. Andreussi, T. Brumme, O. Bunau, M.B. Nardelli, M. Calandra, R. Car, C. Cavazzoni, D. Ceresoli, M. Cococcioni, N. Colonna, I. Carnimeo, A.D. Corso, S. de Gironcoli, P. Delugas, R.A. DiStasio, A. Ferretti, A. Floris, G. Fratesi, G. Fugallo, R. Gebauer, U. Gerstmann, F. Giustino, T. Gorni, J. Jia, M. Kawamura, H.-Y. Ko, A. Kokalj, E. Kucukbenli, M. Lazzeri, M. Marsili, N. Marzari, F. Mauri, N.L. Nguyen, H.-V.Nguyen, A.O. de-la Roza, L. Paulatto, S. Ponce, D. Rocca, R. Sabatini, B. Santra, M. Schlipf, A.P. Seitsonen, A. Smogunov, I. Timrov, T. Thonhauser, P. Umari, N. Vast, X. Wu, S. Baroni. J. Phys. Condens. Matter **29**, 465901 (2017).
[22] S. Tamura. Phys. Rev. B **30**, 849 (1984).
[23] A.P. Zhernov, A.V. Inyushkin. Phys. Usp. **44**, 785 (2001).

Translated by E.Ilyinskaya